NUREG/CR-3857
ANL-84-44

NUREG/CR-3857
ANL-84-44

LONG-TERM EMBRITTLEMENT OF CAST DUPLEX STAINLESS STEELS IN LWR SYSTEMS:

ANNUAL REPORT

October 1982 – September 1983

by

O. K. Chopra and G. Ayrault

ARGONNE NATIONAL LABORATORY, ARGONNE, ILLINOIS
Operated by THE UNIVERSITY OF CHICAGO

Prepared for the Office of Nuclear Regulatory Research
U. S. NUCLEAR REGULATORY COMMISSION
under Interagency Agreement DOE 40-550-75

Argonne National Laboratory, with facilities in the states of Illinois and Idaho, is owned by the United States government, and operated by The University of Chicago under the provisions of a contract with the Department of Energy.

NUREG/CR-3857
ANL-84-44

(Distribution
Code: R5)

ARGONNE NATIONAL LABORATORY
9700 South Cass Avenue
Argonne, Illinois 60439

LONG-TERM EMBRITTLEMENT OF CAST DUPLEX STAINLESS STEELS IN LWR SYSTEMS:

ANNUAL REPORT
October 1982—September 1983

by

O. K. Chopra and G. Ayrault

Materials Science and Technology Division

Report Completed
June 1984

Report Issued
August 1984

Prepared for the Division of Engineering Technology
Office of Nuclear Regulatory Research
U. S. Nuclear Regulatory Commission
Washington, D. C. 20555

NRC FIN No. A2243

LONG-TERM EMBRITTLEMENT
OF CAST DUPLEX STAINLESS STEELS
IN LWR SYSTEMS:

ANNUAL REPORT
October 1982--September 1983

ABSTRACT

This progress report summarizes work performed by Argonne National Laboratory on long-term embrittlement of cast duplex stainless steels in LWR systems during the twelve months from October 1982 to September 1983.

NRC FIN No.	FIN Title
A2243	Long-Term Embrittlement of Cast Duplex Stainless Steels in LWR Systems

TABLE OF CONTENTS

Page

EXECUTIVE SUMMARY iv

I. INTRODUCTION 1

II. TECHNICAL PROGRESS 2

A. Data Review 2

B. Material Procurement 7

C. Microstructural Evaluation 12

REFERENCES 21

LONG-TERM EMBRITTLEMENT
OF CAST DUPLEX STAINLESS STEELS
IN LWR SYSTEMS:

ANNUAL REPORT[a]
October 1982--September 1983

EXECUTIVE SUMMARY

A program has been initiated to investigate the significance of in-service embrittlement of cast duplex stainless steels under LWR operating conditions. The existing data were reviewed to determine the critical parameters that control the aging behavior and to establish test matrices for microstructural studies and mechanical property measurements. Various experimental and commercial heats of CF-8, -8M, and -3 cast stainless steel (ASTM A351 and A451) were procured in different product forms and section thicknesses. The composition of the experimental heats was varied to provide different concentrations of nickel, chromium, carbon, and nitrogen in the material and ferrite contents in the range of 3 to 30 volume percent. Test specimens are being aged at temperatures of 290, 320, 350, 400, and 450°C and for times ranging from 300 to 50,000 h. Material will be available for Charpy impact tests and microstructural studies over the entire range of compositions. A more restricted set of compositions was selected for J_R-curve testing and ductile-to-brittle transition temperature (DBTT) determination. Measurements of impact strength will be used to define the critical parameters that lead to significant embrittlement of the material and to better characterize the phenomenon of embrittlement. Measurements of fracture toughness will be carried out to determine the degree of embrittlement that can be expected under LWR operating conditions.

The initial effort, already begun, is focused on microstructural characterization of aged specimens of CF-8 and CF-8M cast stainless steel, obtained from George Fisher, Ltd. None of the specimens that were aged at temperatures between 300 and 400°C exhibited the mottled structure of α' precipitates. Instead, three different types of precipitates were observed in the specimens: an FCC phase (designated $M_{23}C_6$-like precipitate for lack

[a]RSR FIN Budget No. A2243; RSR Contact: J. Muscara.

of positive identification) present both on and away from dislocations in all long-term-aged specimens, a fine and uniformly distributed precipitate observed in CF-8 (heat 280) stainless steel specimens aged for relatively short times or at low temperature, and a large precipitate observed at the same sites as the $M_{23}C_6$-like precipitates in CF-8M stainless steel specimens. The $M_{23}C_6$-like precipitate may be G phase, a phase rich in nickel and silicon. The microstructural changes in the aged duplex stainless steels indicate a possible correlation between loss of impact strength and degree of precipitation in these specimens.

LONC-TERM EMBRITTLEMENT OF CAST DUPLEX STAINLESS STEELS IN LWR SYSTEMS:

ANNUAL REPORT
October 1982--September 1983

Principal Investigators:
O. K. Chopra and G. Ayrault

I. INTRODUCTION

The primary objectives of this program are (1) to investigate the significance of in-service embrittlement of cast duplex stainless steels under light-water reactor (LWR) operating conditions and (2) to evaluate possible remedies to the embrittlement problem for existing and future plants.

The scope includes the following: (1) characterize and correlate the microstructure of in-service reactor components and laboratory-aged material with loss of fracture toughness and identify the mechanism of embrittlement, (2) determine the validity of laboratory-induced embrittlement data for predicting the toughness of component materials after long-term aging at reactor operating temperatures, (3) characterize the loss of fracture toughness in terms of fracture mechanics parameters in order to provide the data needed to assess the safety significance of embrittlement, and (4) provide additional understanding of the effects of key compositional and metallurgical variables on the kinetics and degree of embrittlement. The kinetics and fracture toughness data generated in this program and from other sources will provide the technical basis for assessing the in-service embrittlement of cast stainless steels under LWR operating conditions. Estimates of the degree of embrittlement will be compared with data obtained from examination of material from actual reactor service. Data pertaining to the effects of compositional and metallurgical variables on the embrittlement phenomenon will help in evaluation of the possible remedies for in-service embrittlement of components in existing and future plants.

II. TECHNICAL PROGRESS

The main areas of effort during the past year have been (a) review of the existing data to determine the critical parameters that control the aging behavior of cast duplex stainless steels and to define the test matrices, (b) procurement of equipment and material, and (c) characterization of the microstructure of material aged at low temperatures for long times.

A. Data Review

Cast duplex stainless steels are used extensively in the nuclear industry. The ferrite phase in the duplex structure of austenitic-ferritic stainless steel increases the tensile strength and improves weldability, resistance to stress corrosion, and soundness of castings of these steels. However, various carbides, brittle chromium-rich phases such as sigma and chi phase, and a chromium-rich BCC phase (α') can precipitate in the ferrite phase or along ferrite/austenite grain boundaries during aging at elevated temperatures. Time-temperature curves[1] for the formation of various phases and the change in impact strengths of Fe-Cr-Ni alloys during aging, shown in Fig. 1, indicate that embrittlement can be divided into two temperature regimes. At temperatures above 550°C, the embrittlement is largely due to formation of σ phase, and below 500°C α' precipitation leads to embrittlement (referred to as "475°C embrittlement"). Formation of carbides and the χ phase can influence mechanical properties in the 500–650°C temperature range. At the operating temperatures of LWRs, i.e., 288 to 316°C, embrittlement of ferritic or duplex stainless steels is usually assumed to be caused primarily by α' precipitation. The influence of carbides/nitrides on the kinetics of the precipitation process and on the subsequent embrittlement of the material cannot be established from the existing experimental data.

Thermal aging of cast duplex stainless steels at temperatures between 300 and 450°C affects the mechanical properties in several ways.[2-6] In general, thermal aging causes an increase in hardness and tensile strength and a decrease in ductility, Charpy impact strength, and J_{IC} fracture toughness of the material. However, the low-cycle fatigue properties and fatigue-crack propagation rates are not modified significantly by aging.[4,5]

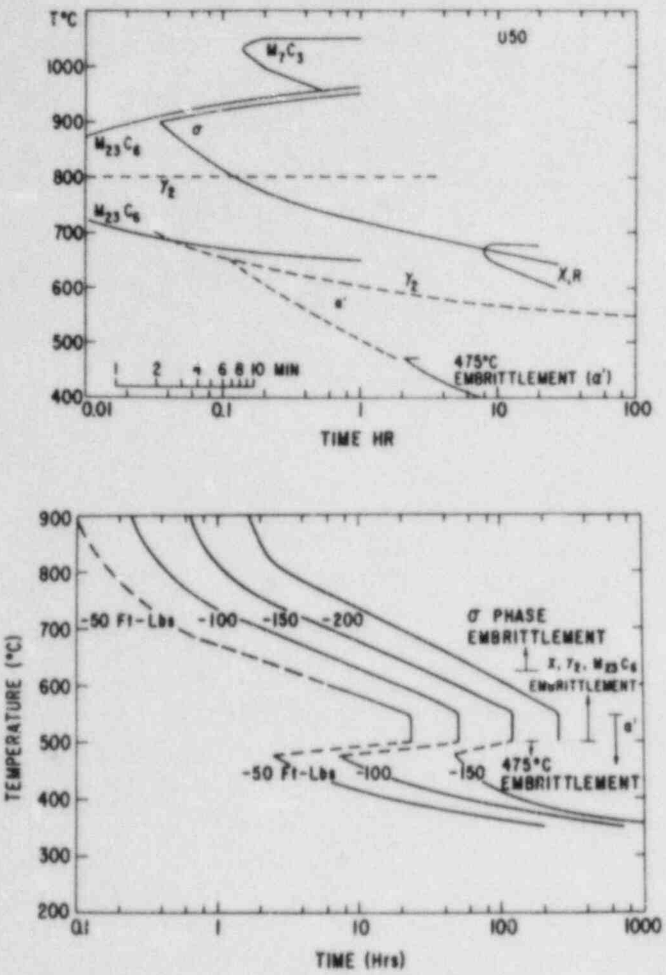

Fig. 1

Time-Temperature Curve for (Top) Formation of Various Phases and (Bottom) Decrease in Room-Temperature Impact Energy in Cast Duplex Stainless Steel. [Solomon and Devine, Ref. 1]

The changes in the tensile strength and room-temperature impact energy for cast CF-8M stainless steel aged for 3000 h at 427°C are shown in Figs. 2 and 3, respectively. The impact strength, in particular, is reduced by ~80%. Substantial reductions in impact strength have also been observed for several CF-8 and CF-8M cast stainless steels after aging for 10,000 to 70,000 h at temperatures as low as 300°C.[2] The ferrite content of the cast structure has a pronounced influence on the embrittlement behavior, viz., an increase in ferrite content increases the susceptibility to embrittlement, as shown in Fig. 4. Also, the addition of molybdenum to the steel, as in grade CF-8M, increases both the rate and extent of embrittlement. The very limited data available on J_{IC} fracture toughness also indicate significant reduction in fracture toughness due to low-temperature aging, although the results do not always show good correlation with the trends indicated by the Charpy data.[5]

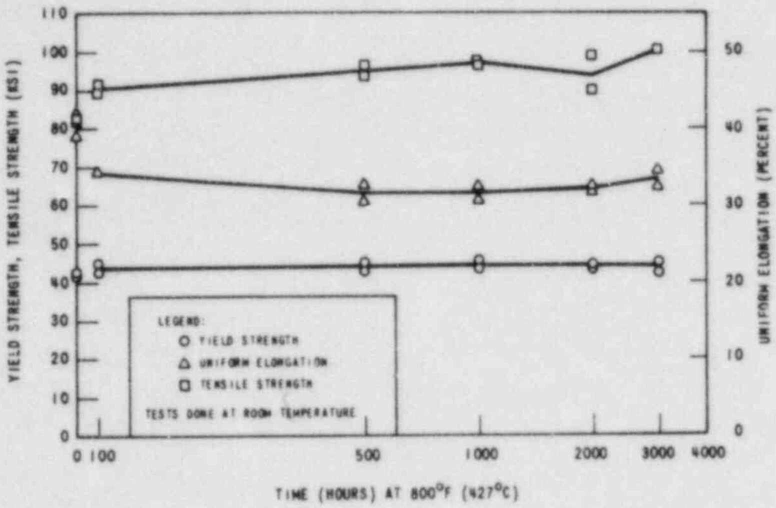

Fig. 2. Tensile Properties of CF-8M (ASTM A451) Cast Stainless Steel after Low-Temperature Aging. [Landermann and Bamford, Ref. 4]

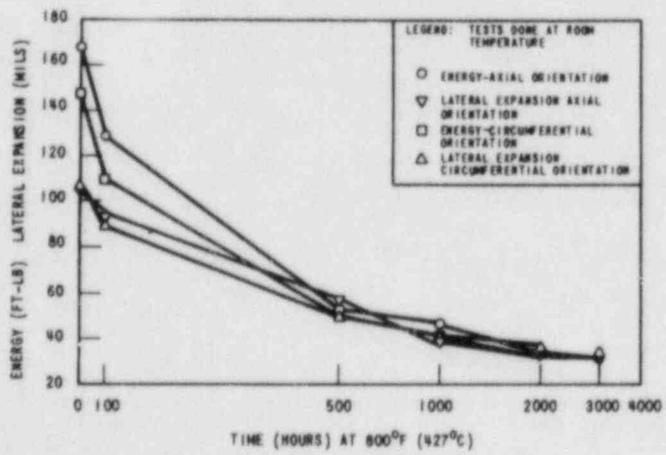

Fig. 3. Decrease in Room-Temperature Impact Energy Due to 475°C Embrittlement of CF-8 (ASTM A451) Cast Stainless Steel. [Landermann and Bamford, Ref. 4]

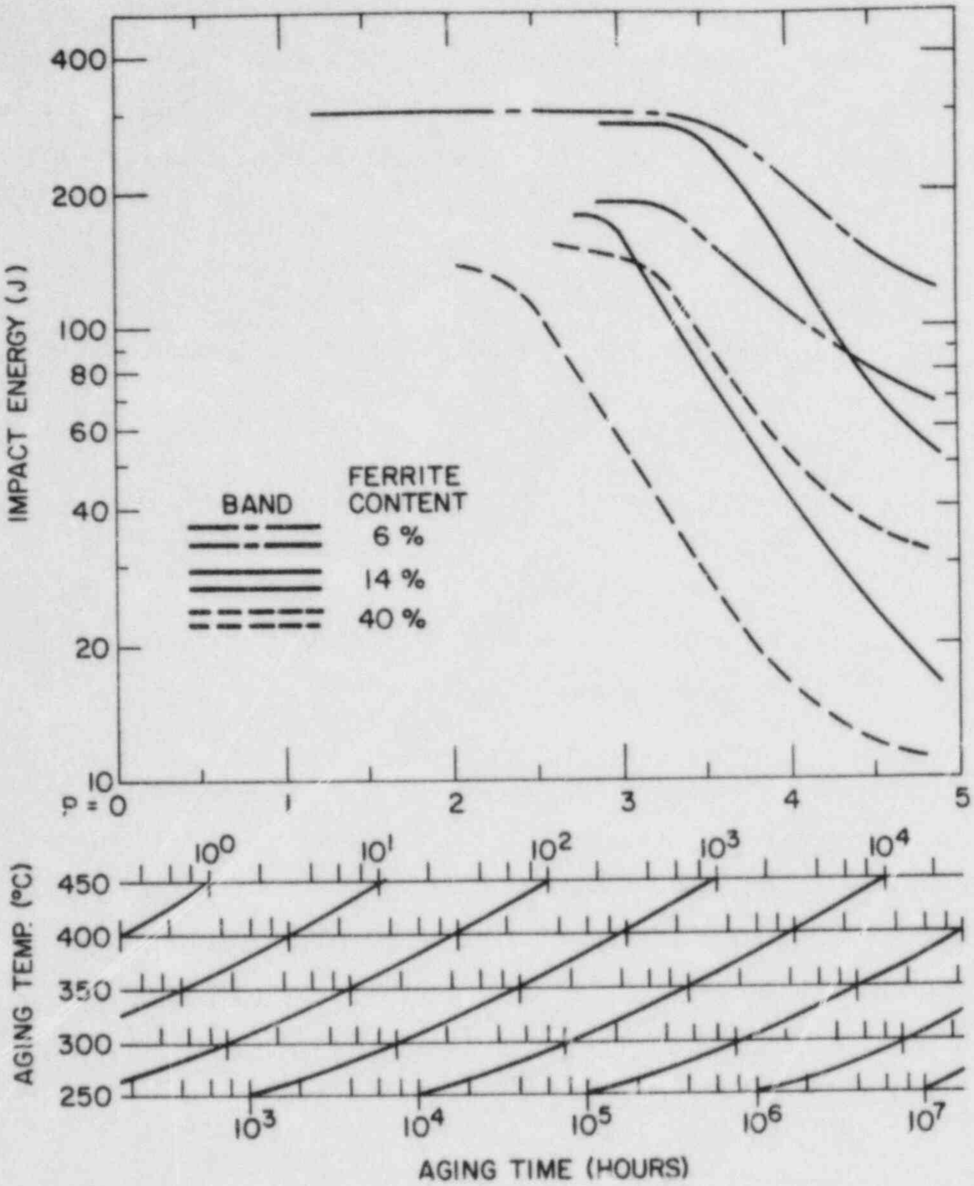

Fig. 4. Influence of Ferrite Content on the Embrittlement of CF-8 and CF-8M (ASTM A351) Cast Stainless Steel. [Trautwein and Gysel, Ref. 2b]

The kinetics of embrittlement have been evaluated by considering the aging phenomenon to be a thermally activated process that can be described by an Arrhenius relation. In the temperature range of 300 to 400°C, the data obtained by George Fisher, Ltd. of Switzerland[2] for thermal aging of various cast duplex stainless steels yields an activation energy of 100 kJ/mole (24,000 cal/mole) for the onset of embrittlement. Extrapolation of the data can be used to determine the equivalent aging time at different temperatures.

For example, a service life of 40 yr at 288 or 316°C, respectively, is equivalent to 10,000 or 28,000 h of aging at 400°C. Based on the Swiss data, the impact energy after the service life at 316°C will be ∿12 J for cast materials with ∿40% ferrite, and ∿28% J for castings containing ∿14% ferrite.[2]

Recent investigations[5] have described the activation energy for the process of embrittlement as a function of chemical composition of the cast material, given by the relationship

$$Q(\text{kJ/mole}) = -182.6 + 19.9\ (\%\ \text{Si}) + 11.08\ (\%\ \text{Cr}) + 14.4\ (\%\ \text{Mo}).$$

The chemical compositions of the various cast materials used by George Fisher, Ltd. yield activation energies between 65 and 90 kJ/mole (∿15 and 22 kcal/mole) for CF-8M cast stainless steel.

More extensive information on the effect of chemical composition on embrittlement of single-phase binary Fe-Cr ferritic alloys is available and is helpful in gaining insight into the effects of composition on aging and in identifying possible mechanisms of embrittlement. Unfortunately, the bulk of this work has been carried out at temperatures of 400°C or above, and caution must be observed in extrapolating the data to reactor temperatures. Data on the thermal aging of single-phase ferritic alloys indicate that an increase in chromium, molybdenum, or titanium content in the ferrite phase decreases the time required for embrittlement.[7] The influence of chromium is more pronounced than that of molybdenum or titanium. Variations in manganese or silicon content have no effect on the aging behavior.[8] For single-phase Fe-Cr-Ni alloys, an increase in the nickel content promotes α' precipitation,[8] but the higher-nickel ferritic steels take longer to embrittle because other deformation modes, such as twinning, are promoted by additions of nickel.[9] Interstitial elements such as carbon and nitrogen also accelerate embrittlement of single-phase ferritic steels. Nitrogen in the ferrite phase influences the aging behavior by enhancing the precipitation of the α' phase and by the formation of nitrides or carbonitrides.[7,10-12]

To demonstrate the validity of an Arrhenius extrapolation to predict the long-term embrittlement of steels at reactor operating temperatures, a satisfactory understanding of the aging process and the mechanism of embrittlement is required to ensure that the activation energy obtained from the laboratory tests is representative of the actual process. The value of activation energy determined from the aging data is much lower than that expected for a mechanism controlled by solute bulk diffusion (i.e., activation energy of 54,900 cal/mole). This indicates that α' precipitation occurs not via nucleation and growth but by another mechanism, e.g., spinodal decomposition, or that processes other than α' precipitation contribute to embrittlement. The available information on the microstructure of aged cast duplex stainless steels is not sufficient for correlating the microstructure with the mechanical properties or for determining the mechanism of low-temperature embrittlement.

B. Materials Procurement

Material was obtained from various experimental and commercial heats of CF-8, -8M, and -3 (ASTM A351 and A451) cast stainless steel in different product forms and section thicknesses. Nineteen experimental heats of cast stainless steel material were obtained in the form of keel blocks. The composition was varied to provide different concentrations of nickel, chromium, carbon, and nitrogen in the material and ferrite contents in the range of 3 to 30%. Sections from five different centrifugally cast pipes (grades CF-8 and CF-8M), a pump impeller, and a pump casing ring (grade CF-8) were also procured. The outer diameter and wall thickness of the cast pipes range from 0.6 to 0.9 m and 38.1 to 76.2 mm, respectively. Material will be available for Charpy impact tests and microstructural studies over the entire range of compositions. However, it is prohibitively expensive to procure and age material for J_R curve testing for all compositions. Therefore, a more restricted set of compositions was selected for these tests. The material will be obtained from large heats (~2000 lb) in the form of 76-mm-thick slabs. The test matrix for the microstructural studies and mechanical property measurements is given in Table 1.

TABLE 1. Test Matrix for CF-8 and CF-8M Cast Stainless Steel Specimens

Material	Metallurgical Characterization[a]	TEM & Neutron Diffraction	Charpy Impact	Hardness	Instrumented Impact	DBTT	J_R Curve[b]
Swiss impact specimens	x	x					
In-service components	x	x	x	x			x
Large heats[c]	x		x	x	x	x	x
Reactor components[c]	x	x	x	x	x	x	x
Small heats[c]	x	x	x	x			

aracterization of chemical composition, ferrite content, and grain size and structure.

[b]2T compact tension specimens will be used for the large heats and 1T compact tension specimens will be used for reactor components.

[c]Tests will be performed after thermal aging.

Facilities for conducting long-term aging of cast material for Charpy impact and compact tension specimens have been completed. Preliminary tests were carried out to determine the temperature gradient in the furnaces and the accuracy of temperature control. The furnaces were lined with steel shells to increase the heat capacity and the size of the uniform-temperature zone. Charpy impact specimen blanks were prepared from keel blocks of the experimental heats and material from the various reactor components. Blanks for 1-T compact tension specimens were obtained from sections of two centrifugally cast pipes, a static-cast pump casing ring, and the pump impeller. The orientations and locations of the mechanical test specimens are shown in Fig. 5. The aging conditions for the various specimens are given in Table 2. The effects of aging time and temperature on the formation of precipitates and the onset of embrittlement will be determined by microstructural examination, hardness measurements, and Charpy impact tests. Measurements of impact strength and DBTT will be used to define the aging histories, chemical compositions, and metallurgical structures that lead to significant embrittlement. Fracture toughness tests will be carried out to determine the degree of embrittlement that can be expected as a function of service time and the compositional variables.

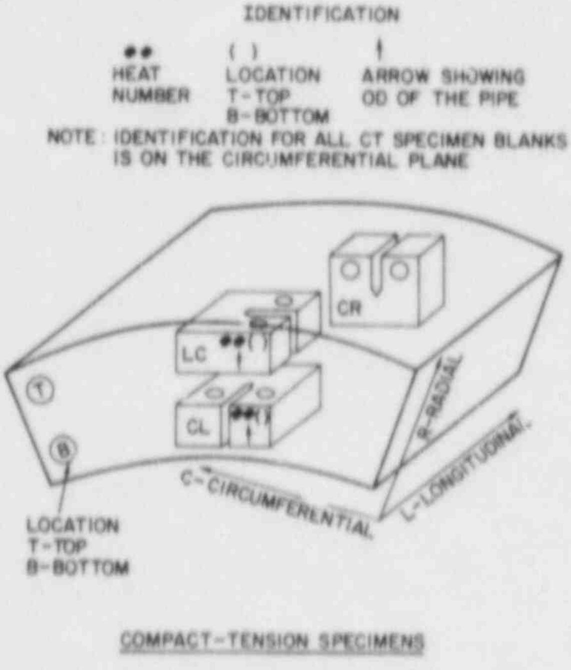

(a)

Fig. 5. Orientation and Location of the Mechanical Test Specimens Taken from (a and b) Pipe Sections and (c) Keel Blocks.

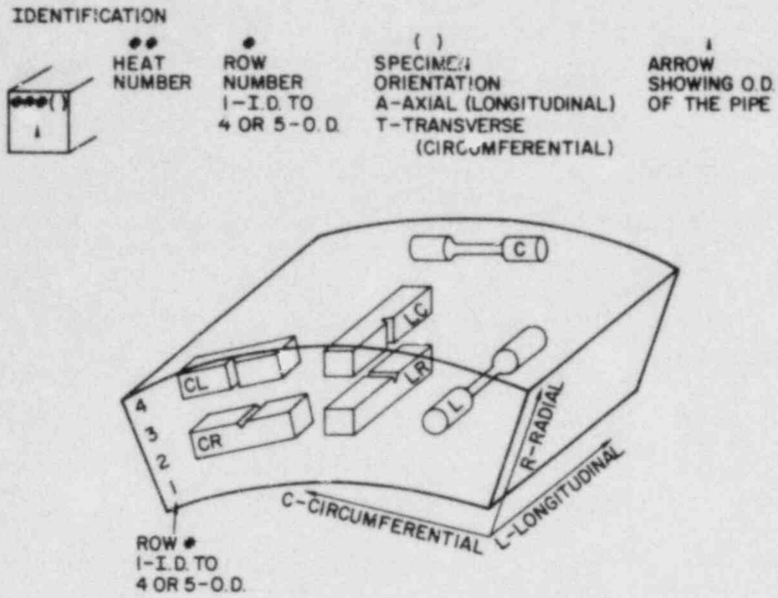

CHARPY IMPACT AND TENSILE SPECIMENS

(b)

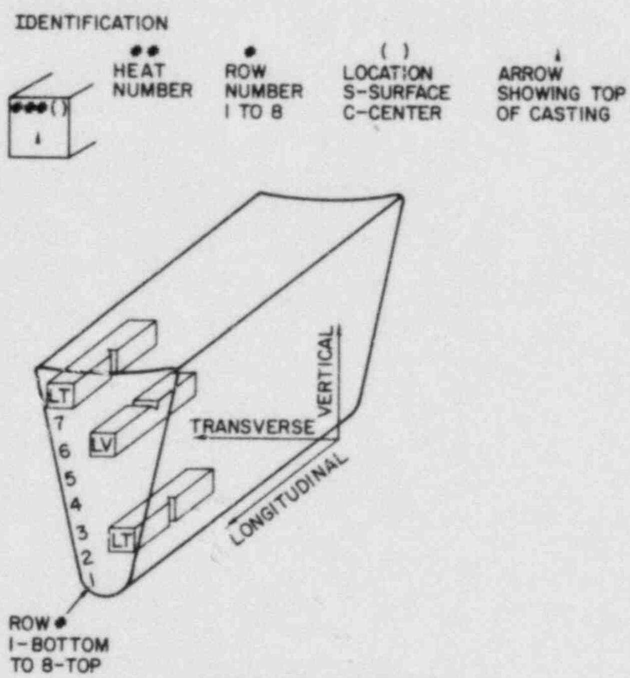

CHARPY IMPACT SPECIMENS

(c)

Fig. 5. (Contd.)

TABLE 2. Aging Time and Temperature for Cast Materials Used in Charpy Impact and J-Integral Tests

Time, h	Temperature, °C				
	450	400	350	320	290
100	a	a			
300	a	a	a		
1,000	a	a	a	a	
3,000	a	a	a,b	a	a
10,000	a	a,b	a,b,c	a,b	a
30,000	a	a	a,b,c	a,b,c	a,b,c
>50,000		a	a	a,b	a,b

[a] Charpy impact test at room temperature on experimental heats (4 specimens in each condition) and reactor components (3 axial and 2 transverse specimens in each condition).

[b] 1. Instrumented Charpy impact test at room temperature on experimental heats and reactor components (2 axial specimens in each condition). 2. J-Integral test at room temperature on reactor components (1 transverse and 2 axial specimens in each condition).

[c] 1. Charpy impact test at 7 temperatures (DBTT) on reactor components (14 axial specimens in each condition). 2. J-Integral test at 290°C on reactor components (2 axial specimens in each condition).

Characterization of the various cast materials is in progress to determine the chemical composition, ferrite content, hardness, and grain structure. The ferrite content and hardness of the material from cast keel blocks and components are given in Table 3. A ferrite scope (Auto Test FE, Probe Type FSP-1) was used to measure the ferrite content of the castings. The accuracy of the instrument was checked with several weld-metal standards (ferrite numbers between 2.4 and 28.1) obtained from the British Welding Institute. The ferrite numbers measured with the ferrite scope were within

±0.2 of the standard values for ferrite numbers up to 13, and were ~10% higher than the standards for ferrite numbers >16. For each heat of the cast material, hardness and ferrite content were measured in three orientations, i.e., in the axial, circumferential, and radial planes, as well as different locations, namely, regions near the outer surface, center, and inner surface of the pipes, and near the top and bottom of the keel blocks. Average values of all the measurements (~60) are given in Table 3. In general, the ferrite content was lower and hardness was slightly higher towards the inner surface of the pipes and the top sections of the cast keel blocks. The hardness of the cast material increased with an increase in ferrite content. For the same ferrite content, the hardnesses of CF-8 and CF-8M material were comparable, but the hardnesses of both were higher than that of cast CF-3 material. The orientation of the specimen had relatively little effect on the hardness and ferrite content. Characterization of the grain structure, chemical composition, and microhardness of the materials is in progress.

C. Microstructural Evaluation

The microstructural studies were focused on cast duplex stainless steel aged in the laboratory at low temperatures for long times. Twenty fractured impact bars from three heats of aged cast duplex stainless steel (grades CF-8 and CF-8M) were obtained from George Fisher, Ltd. The material was used earlier to study the long-term aging behavior of cast stainless steels.[2] The specimens from CF-8 material (heats 278 and 280) were aged for 3000, 10,000, and 70,000 h at 300, 350, and 400°C, while the specimens from CF-8M material (heat 286) were aged for 1000 and 10,000 h at 400°C.

Two ferritic alloys, 26Cr-1Mo and 29Cr-4Mo-2Ni, and a cast duplex stainless steel (heat B) were used to develop the technique for preparing TEM samples from the cast materials. The ferritic alloys were supplied by Allegheny Ludlum Steel Corp., and have been used in a study of the 475°C embrittlement phenomenon at temperatures between 371 and 593°C.[13] The chemical compositions of the various steels used for microstructural examination are given in Table 4. Material from the two ferritic alloys and cast stainless steel (heat B) was aged for 100 and 1000 h at 400 and 475°C for TEM inspection.

TABLE 3. Chemical Composition, Hardness, and Ferrite Content of the Various Heats of Cast Stainless Steel

Heat	Grade	Composition,[a] wt.%							Hardness R_B	Ferrite Content,[b] %
		Mn	Si	Mo	Cr	Ni	N	C		
					Cast Keel Blocks					
58	CF-8	0.66	1.21	0.29	19.56	10.37	0.040	0.05	77.1 ± 1.9	2.9 ± 1.1
57		0.69	1.24	0.28	18.45	8.94	0.041	0.06	80.1 ± 1.0	4.3 ± 1.3
54		0.58	1.08	0.31	19.42	8.91	0.073	0.065	83.3 ± 1.0	-
53		0.70	1.28	0.35	19.62	8.86	0.045	0.07	83.1 ± 0.9	8.6 ± 1.1
56		0.60	1.16	0.30	19.33	8.93	0.031	0.06	82.5 ± 1.4	10.0 ± 2.3
59		0.63	1.14	0.26	20.35	8.95	0.040	0.07	84.1 ± 1.7	13.5 ± 1.1
61		0.70	1.20	0.27	20.54	8.59	0.060	0.06	85.3 ± 1.0	13.1 ± 0.8
60		0.71	1.01	0.26	21.02	8.07	0.050	0.07	86.7 ± 0.6	21.0 ± 1.2
50	CF-3	0.67	1.26	0.28	17.63	8.84	0.064	0.019	80.1 ± 1.0	4.3 ± 0.9
49		0.66	1.11	0.29	19.32	10.10	0.064	0.022	76.7 ± 1.3	7.1 ± 1.1
48		0.67	1.21	0.26	19.42	9.90	0.071	0.016	78.1 ± 0.8	8.7 ± 0.5
47		0.65	1.23	0.45	19.67	10.04	0.027	0.018	79.7 ± 0.9	16.3 ± 0.9
52		0.63	1.04	0.31	19.51	9.07	0.049	0.021	81.6 ± 0.8	13.5 ± 3.6
51		0.66	1.06	0.28	20.36	8.69	0.048	0.023	83.8 ± 0.5	18.0 ± 0.9
62	CF-8M	0.84	0.64	2.46	18.38	11.35	0.030	0.07	78.1 ± 1.0	4.4 ± 2.3
63		0.69	0.75	2.52	19.39	11.22	0.030	0.05	81.6 ± 1.0	10.4 ± 0.7
66		0.71	0.60	2.36	19.41	9.13	0.030	0.06	85.2 ± 1.1	19.8 ± 0.7
65		0.66	0.63	2.53	20.95	9.39	0.060	0.06	89.0 ± 0.8	23.4 ± 2.3
64		0.70	0.71	2.41	20.87	9.01	0.030	0.05	89.7 ± 0.6	28.4 ± 1.1
					Cast Components					
P3	CF-8	1.13	0.91	0.01	19.05	8.94	0.21	0.033	81.9 ± 2.9	2.1 ± 0.9
C1		1.13	1.08	-	19.30	8.90	-	0.06	79.2 ± 1.5	3.5 ± 0.5
P1		-	-	-	-	-	-	-	84.8 ± 1.1	24.2 ± 3.8
P2	CF-3	0.83	1.02	0.11	20.09	9.64	-	0.027	80.9 ± 6.2	15.7 ± 2.2
P4	CF-8M	1.12	1.00	2.37	20.20	10.22	0.17	0.044	83.1 ± 1.0	10.5 ± 0.8

[a]Chemical compositions obtained from the vendor.

[b]Ferrite content measured by ferrite scope (Auto Test FE, Probe Type FSP-1).

TABLE 4. Chemical Compositions of Steels Used for Microstructural Evaluation

Designation		Composition, wt %									Ferrite Content, %	
Heat	Grade	Mn	Si	Mo	Cr	Ni	P	S	N	C	Calc.[a]	Meas.
						Cast Stainless Steel						
B	CF-8A	0.89	1.34	0.52	21.13	8.44	0.019	0.014	0.165	0.046	9.2	-
278[b]	CF-8	0.28	1.00	0.13	20.20	8.27	0.008	0.019	0.027	0.038	19.00	15
280[b]	CF-8	0.50	1.37	0.25	21.60	8.00	0.015	0.006	0.029	0.028	38.7	38
286[b]	CF-8M	0.40	1.33	2.44	20.20	9.13	0.044	0.015	0.063	0.072	18.8	22
						Ferritic Steel						
26-1S	-	-	-	0.97	26.0	0.14	-	-	0.019	0.030	-	-
29-4-2	-	-	-	3.90	29.6	2.20	-	-	0.011	0.006	-	-

[a]Calculated from composition with hulls equivalent factor.
[b]Heats obtained from George Fisher, Ltd.

Aging of the CF-8 cast stainless steel (heat B) for 1000 h at 475°C produced two different types of precipitates in the ferrite grains. A general precipitate was distributed uniformly in the ferrite grains; another was found only on dislocations. Neither of the precipitates was present in the unaged specimens. The general precipitate had a mottled or "orange peel" appearance in bright-field images, shown in Fig. 6a, but produced no detectable changes in diffraction patterns. Such micrographs are generally accepted as evidence of the chromium-rich α' precipitates. The mottled-contrast images seen in duplex stainless steel and in a Fe-46Cr alloy were shown (by Mossbauer spectroscopy[8] and precipitate extraction techniques,[9] respectively) to be due to the α' precipitate. The precipitates formed on the dislocations (Fig. 6b) were typically 15- to 40-nm cubes with {100} matrix planes as faces. These precipitates were not α' and exhibited a distinct diffraction pattern consistent with an FCC structure similar to $M_{23}C_6$ patterns, but with a slightly large lattice parameter. The precipitates also had a cube-on-cube orientation relative to the BCC ferrite matrix, which would be unusual for $M_{23}C_6$ phase. Preliminary energy-dispersive X-ray analyses indicated an enrichment of nickel and silicon in these precipitates. These results suggest that the precipitates are probably G phase (a phase rich in Ni and Si), which has been observed in Fe-12Cr-4Ni alloy after aging at 450°C[14] and in commercial EM-12 (9Cr-2Mo), HT-9 (12Cr-1Mo), and AISI 416

(13Cr) ferritic steels after irradiation at temperatures below 425°C.[15] Until a more positive identification can be made, these precipitates will be designated as $M_{23}C_6$-like precipitates.

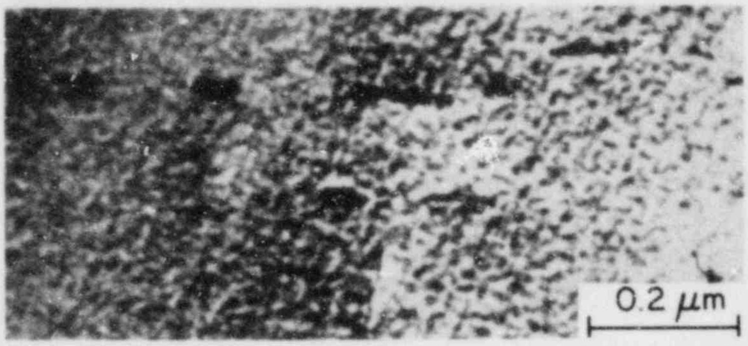

(a)

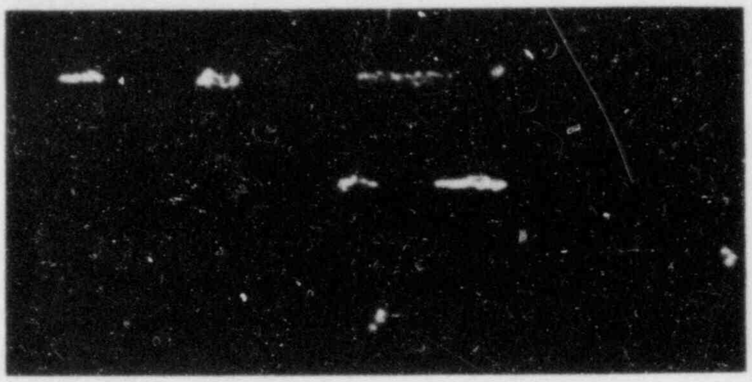

(b)

Fig. 5. Precipitation in CF-8 (ASTM A351) Cast Stainless Steel Aged for 1000 h at 475°C. (a) Bright-field image under (110) two-beam diffraction conditions, and (b) dark-field image from the (333) reflection in the FCC precipitate diffraction pattern.

Aging of the two single-phase ferritic alloys, 26Cr-1Mo and 29Cr-4Mo-2Ni, for 1000 h at 475°C also produced the mottled bright-field images associated with the α' precipitates. In addition, platelet precipitates were observed in the 29Cr-4Mo-2Ni alloy. The precipitate microstructure of the ferritic alloys is essentially identical to that reported in an earlier study.[13] The diffraction patterns and the contrast images of the platelets suggest that they are not α' or the $M_{23}C_6$-like precipitates. Aging for 1000 h at 400°C produced no obvious microstructural changes in CF-8 cast stainless steel and the 26Cr-1Mo ferritic alloy, whereas platelet precipitates were observed in the 29Cr-4Mo-2Ni ferritic alloy.

TEM examination of the aged specimens of cast duplex stainless steel obtained from George Fisher, Ltd. did not reveal the mottled images of α' precipitates. The CF-8 stainless steel, heat 280 (containing 40% ferrite), aged for 66,650 h at 400°C, underwent profuse precipitation in the ferrite grains, both at and away from dislocations, as shown in the images in Fig. 7. These precipitates were similar to the $M_{23}C_6$-like precipitates observed in heat B, which was aged for 1000 h at 475°C. Precipitates that formed on the dislocations were about 15 nm in diameter and those away from dislocations were ∿5 nm in size. The diffraction pattern, shown in Fig. 8, indicates an FCC unit cell with a cube-on-cube orientation with the ferrite matrix. The precipitate unit cell is a factor of about 3.95 larger than that of the ferrite matrix. These precipitates were not present after aging for 10,000 h at 400°C. Another type of precipitate was observed on the dislocations, as shown in Fig. 9. This precipitate, however, could not be identified; the precipitate re⁻lections were too weak, owing to the low volume fraction of the precipitate, and were streaked as a result of the small particle size. This fine-size precipitate was the only precipitate present in the specimens of heat 280, which were aged for 70,000 h at 300°C.

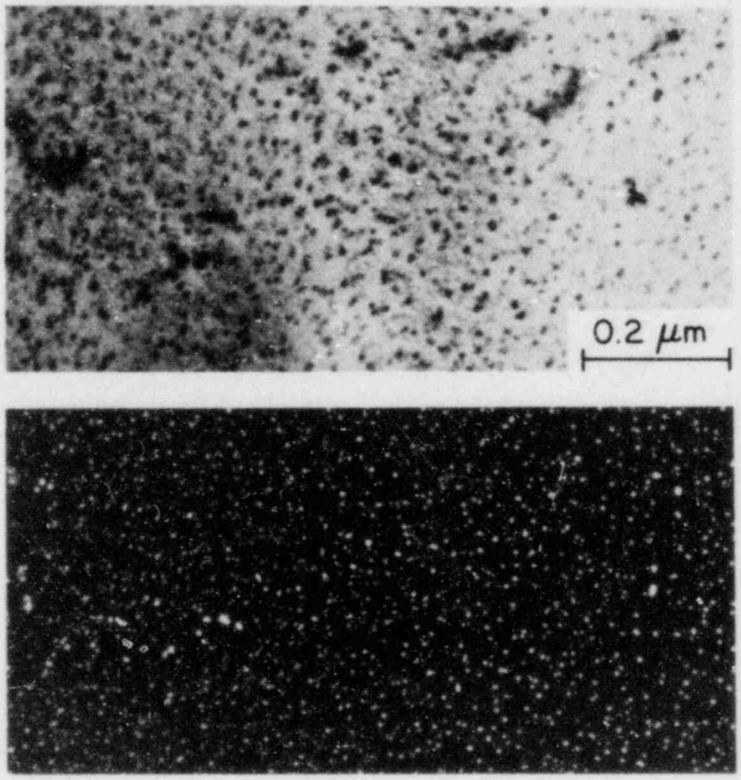

Fig. 7. Bright- and Dark-Field Images of Precipitates in the Ferrite Phase of CF-8 Stainless Steel (Heat 280) Aged for 66,650 h at 400°C.

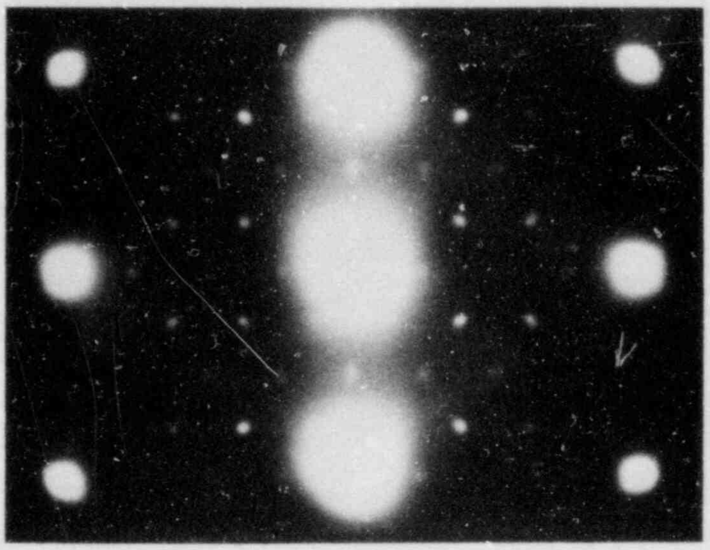

Fig. 8. Selected Area Diffraction Pattern at (110) Orientation in CF-8 Stainless Steel (Heat 280) Aged for 66,650 h at 400°C.

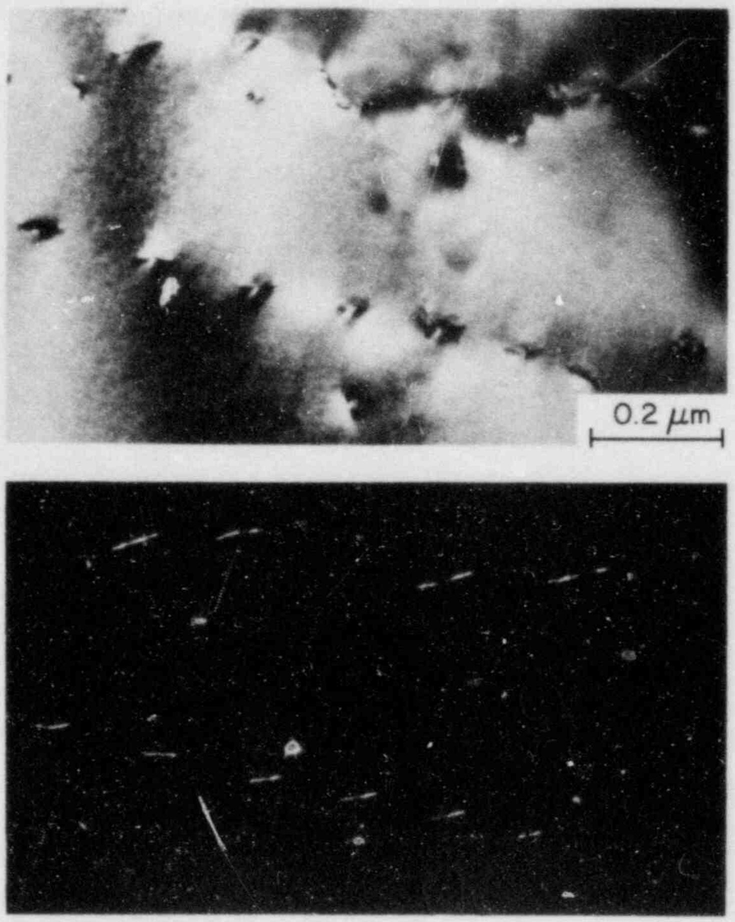

Fig. 9. Bright- and Dark-Field Images of Precipitates in CF-8 Stainless Steel (Heat 280) Aged for 10,000 h at 400°C.

Examination of heat 278 (containing 15% ferrite) of CF-8 cast stainless steel, which was aged for ∿70,000 h at 400°C, also revealed the $M_{23}C_6$-like precipitates; however, their distribution was somewhat different than that in heat 280. In heat 278 the precipitates on dislocations tended to be larger whereas those away from dislocations were smaller. Furthermore, it was clear from diffraction pattern intensities of the precipitates that heat 278 had a lower volume fraction of precipitates than heat 280. Heat 278 was found to embrittle more slowly than heat 280 in tests performed by George Fisher, Ltd.[2] The different distribution of precipitate phases suggests that the greater ferrite content is not the only reason for rapid embrittlement of heat 280. The $M_{23}C_6$-like precipitates were also observed in heat 278 after aging for 70,000 h at 300°C, as shown in Fig. 10. This same heat treatment did not produce $M_{23}C_6$-like precipitates in heat 280. These results indicate that small changes in alloy chemistry not only affect the ferrite content but also influence the precipitation behavior.

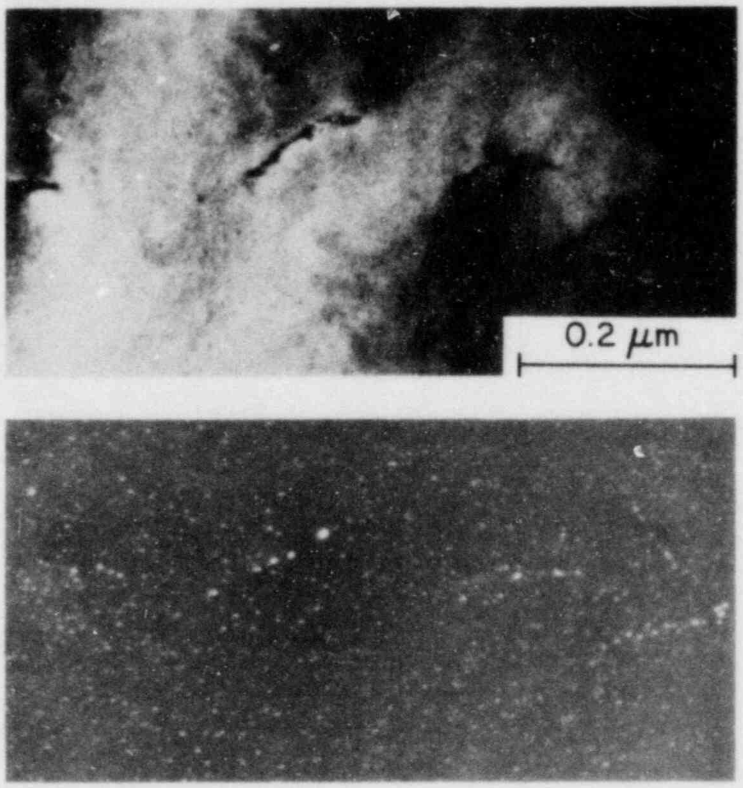

Fig. 10. Bright- and Dark-Field Images of Precipitates in CF-8 Stainless Steel (Heat 278) Aged for 70,000 h at 300°C.

Microstructural evaluation of aged CF-8M stainless steel also indicates that the embrittlement behavior is related to precipitate morphology and distribution. Data obtained on the long-term aging behavior of cast duplex stainless steels[2] indicate that the loss of impact strength of CF-8M (heat 286) after aging for 10,000 h at 400°C is equivalent to that for the CF-8 (heat 280) after aging for 66,650 h at 400°C. TEM examination of CF-8M stainless steel (heat 286), aged for 10,000 h at 400°C, revealed profuse intragranular precipitates both at and away from dislocations, as shown in Fig. 11. The degree of precipitation in the CF-8M specimen is comparable to that in heat 280 aged for 66,650 h at 400°C and much greater than that in heat 278 aged for 66,650 h at 400°C. Diffraction patterns of the specimen indicate that the $M_{23}C_6$-like precipitates are about 3 nm in diameter, as shown in Fig. 11b. However, intense reflections were also observed near the {333} and {115} FCC precipitate reflections, which produced larger (~5 nm) images at the same sites as the images from the FCC reflections, as shown in Fig. 11c. These larger precipitates form a virtual coating on dislocations and should therefore be effective in dislocation pinning. It is not yet clear whether the larger precipitates simply nucleate at the sites of the smaller precipitates or form by transformation of the FCC precipitate phase. A more detailed inspection of these specimens and the specimens aged at 350°C is in progress.

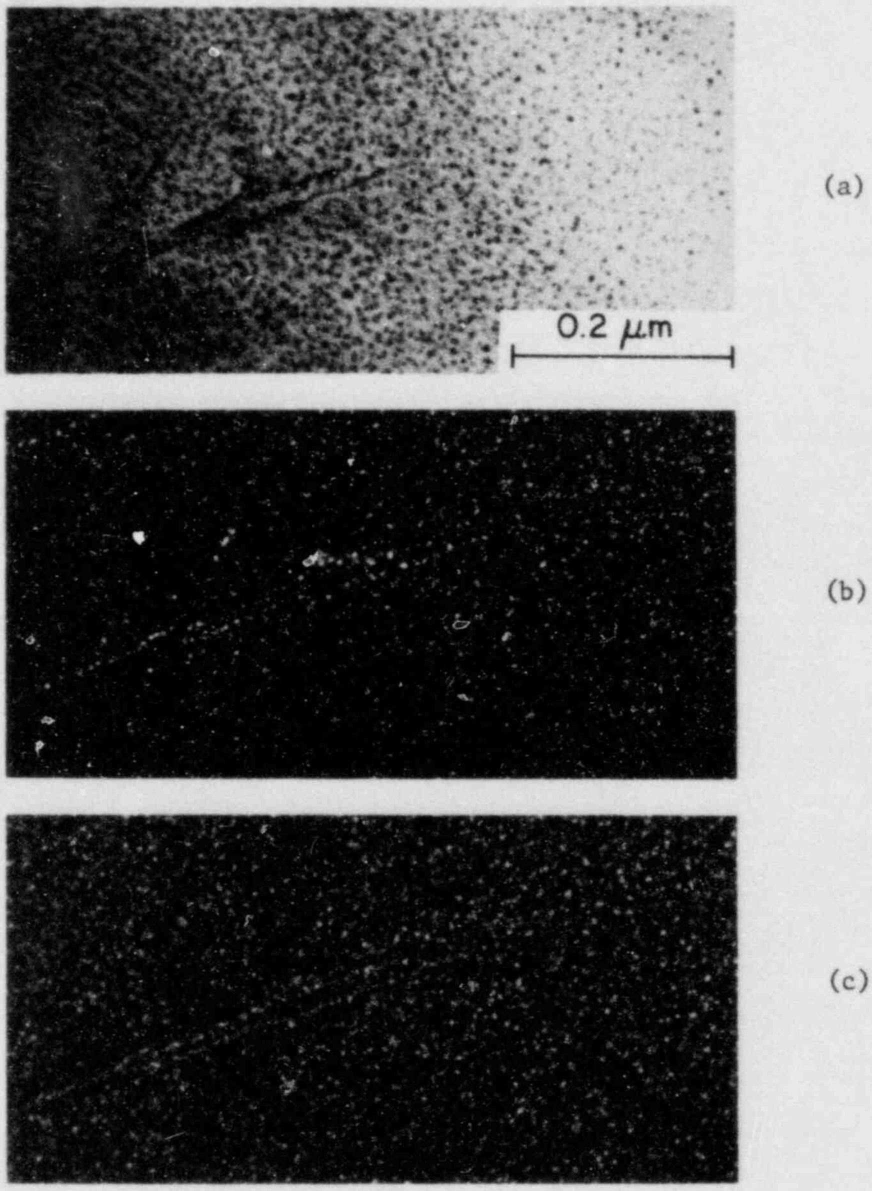

Fig. 11. Precipitates in CF-8M Stainless Steel (Heat 286) Aged for 10,000 h at 400°C. (a) Bright field, (b) dark field using {600} precipitate reflections, and (c) dark field using {115} precipitate reflections.

REFERENCES

1. H. D. Solomon and T. M. Devine, "Influence of Microstructure on the Mechanical Properties and Localized Corrosion of a Duplex Stainless Steel," in MiCon 78: Optimization of Processing, Properties, and Service Performance Through Microstructural Control, eds. Abrams, Maniar, Nail and Solomon, ASTM STP 672 (1979), p. 430.

2. A. Trautwein and W. Gysel, (a) "Influence of Long Time Aging of CF8 and CF8M Cast Steel at Temperatures Between 300 and 500 Deg. C on the Impact Toughness and the Structure Properties," Spectrum, Technische Mitteilungen aus dem+GF+Konzern, No. 5, May 1981; Stainless Steel Castings, eds. V. G. Behal and A. S. Melilli, ASTM STP 756 (1982), p. 165; (b) Figure in EPRI NP-2705-SR (October 1982), p. 3.18.

3. G. Baudry and C. Pichard, "Evolution During Long Holding Times at 300 and 450°C of the Mechanical Properties of Austeno-Ferritic Steel Castings and Welded Joints Used in Pressurized Water Nuclear Reactors," Troisieme Congres National Sur La Technologie Des Appareils a Bression, Vol. 2, Materiaux, A.F.I.A.P. (1980), p. 673.

4. E. I. Landerman and W. H. Bamford, Fracture Toughness and Fatigue Characteristics of Centrifugally Cast Type 316 Stainless Steel Pipe after Simulated Thermal Service Conditions, Ductility, and Toughness Considerations in Elevated Temperature Service, ASME MPC-8 (1978), p. 99.

5. G. Slama, P. Petrequin, and T. Magep, "Effect of Aging on Mechanical Properties of Austenitic Stainless Steel Castings and Welds," presented at SMIRT Post-Conference Seminar 6, Assuring Structural Integrity of Steel Reactor Pressure Boundary Components, Monterey, CA, Aug. 29-30, 1983.

6. W. H. Bamford, E. I. Landerman, and E. Diaz, "Thermal Aging of Cast Stainless Steel and Its Impact on Piping Integrity," presented at ASME National Congress on Pressure Vessels and Piping, Portland, Oregon, 1983.

7. P. J. Grobner, The 885°F (475°C) Embrittlement of Ferritic Stainless Steel, Metall. Trans. 4, 251 (1973).

8. H. D. Solomon and L. M. Levinson, Mossbauer Effect Study of 475°C Embrittlement of Duplex and Ferritic Stainless Steels, Acta Metall. 26, 492 (1978).

9. M. J. Marcinkowski, R. M. Fisher, and A. Szirmae, Effect of 500°C Aging on the Deformation Behavior of an Iron-Chromium Alloy, Trans. AIME 230, 676 (1964).

10. A. Hendry, Z. F. Mazur, and K. H. Jack, Influence of Nitrogen on 475°C Embrittlement of High-Chromium Ferritic Steels, Met. Sci. 13, 482 (1979).

11. M. Courtnall and F. B. Pickering, The Effect of Alloying on 475°C Embrittlement, Met. Sci. 10, 273 (1976).

12. R. Lagneborg, Metallography of the 475°C Embrittlement in an Iron-30% Chromium Alloy, Trans. ASM 60, 67 (1967).

13. T. J. Nichol, A. Dalta, and G. Aggen, Embrittlement of Ferritic Stainless Steels, Metal. Trans. 11A, 573 (1980).

14. G. T. Brown and R. T. Allsop, Embrittlement of a 12%Cr-4Ni Steel, J. Iron Steel Inst. (1960), p. 435.

15. D. S. Gelles and L. E. Thomas, "Effects of Neutron Irradiation on Microstructure in Commercial and Experimental Ferritic Alloys," presented at the Topical Conf. on Ferritic Alloys for Use in Nuclear Energy Technologies, Snowbird, Utah, June 19-23, 1983.

Distribution for NUREG/CR-3857 (ANL-84-44)

Internal:

R. Avery
G. Ayrault
O. K. Chopra (5)
H. M. Chung
D. R. Diercks
F. Y. Fradin
T. F. Kassner (5)
K. L. Kliewer
D. S. Kupperman
D. K. Moores
F. A. Nichols
J. Y. Park
W. J. Shack (3)
W. K. Soppet
E. M. Stefanski (2)
C. E. Till
R. A. Valentin
R. W. Weeks
H. Wiedersich
R. S. Zeno
ANL Patent Dept.
ANL Contract File
ANL Libraries (3)
TIS Files (6)

External:

NRC, for distribution per R5 (350)
DOE-TIC (2)
Manager, Chicago Operations Office, DOE
R. Tom, DOE-CH
Materials Science and Technology Division Review Committee:
B. Alcock, U. Toronto
A. Arrott, Simon Fraser U.
R. C. Dynes, Bell Labs., Murray Hill
A. G. Evans, U. California, Berkeley
L. M. Falicov, U. California, Berkeley
H. K. Forsen, Bechtel Group, San Francisco
E. Kay, IBM San Jose Research Lab.
B. Maple, U. California, San Diego
C. L. McCabe, Cabot Corp., Kokomo, Ind.
P. G. Shewmon, Ohio State U.
J. Tien, Columbia U.
G. A. Arlotto, Office of Nuclear Regulatory Research, USNRC, Washington
D. Atteridge, Battelle Pacific Northwest Lab., P. O. Box 999, Richland, Wash. 99352
W. H. Bamford, Structural Materials Engineering, Westinghouse Electric Corporation, WNES, Box 355, Pittsburgh, PA 15230
C. Y. Cheng, Office of Nuclear Reactor Regulation, USNRC, Washington
W. J. Collins, Office of Inspection and Enforcement, USNRC, Washington
A. Cowan, Risley Nuclear Power Development Labs., United Kingdom Atomic Energy Authority (Northern Division), Risley, Warrington WA3 6AT, UK
W. H. Cullen, Materials Engineering Associates, Inc., 9700 B George Palmer Highway, Lanham, Maryland 20706
B. J. L. Darlaston, CEGB, Berkeley Nuclear Laboratories, Berkeley, Glos., England
B. J. Elliot, Office of Nuclear Reactor Regulation, USNRC, Washington
W. Gysel, George Fischer, Ltd., Schaffhausen, Switzerland
W. S. Hazelton, Office of Nuclear Reactor Regulation, USNRC, Washington
B. Hemsworth, HM Nuclear Installations Inspectorate, Thames House North, Millbank, London SW1P 42J, England
W. V. Johnston, Office of Nuclear Reactor Regulation, USNRC, Washington
P. M. Lang, Office of Converter Reactor Deployment, USDOE, Washington, D. C. 20545

J. Muscara, Office of Nuclear Regulatory Research, USNRC, Washington
D. M. Norris, Electric Power Research Inst., P. O. Box 10412, Palo Alto, Calif. 94304
C. Z. Serpan, Office of Nuclear Regulatory Research, USNRC, Washington
V. K. Sikka, Oak Ridge National Laboratory, P. O. Box X, Oak Ridge, TN 37830
G. Slama, Framatome, Tour FIAT, Cedex 16, 92084, Paris La Defense, France
P. Smerd, Combustion Engineering, Inc., P. O. Box 500, Windsor, Conn. 06095
H. D. Solomon, General Electric Co., P. O. Box 43, Schenectady, NY 12301
D. M. Stevens, Lynchburg Research Center, Babcock & Wilcox Co., P. O. Box 239, Lynchburg, VA 24505-0239
J. Strosnider, Office of Nuclear Regulatory Research, USNRC, Washington

NRC FORM 335 (11-81) U.S. NUCLEAR REGULATORY COMMISSION **BIBLIOGRAPHIC DATA SHEET**	1. REPORT NUMBER (Assigned by DDC) NUREG/CR-3857 (ANL-84-44)
4. TITLE AND SUBTITLE (Add Volume No., if appropriate) LONG-TERM EMBRITTLEMENT OF CAST DUPLEX STAINLESS STEELS IN LWR SYSTEMS: ANNUAL REPORT, October 1982--September 1983	2. (Leave blank)
	3. RECIPIENT'S ACCESSION NO.
7. AUTHOR(S) O. K. Chopra and G. Ayrault	5. DATE REPORT COMPLETED MONTH June YEAR 1984
9. PERFORMING ORGANIZATION NAME AND MAILING ADDRESS (Include Zip Code) Argonne National Laboratory 9700 S. Cass Avenue Argonne, Illinois 60439	DATE REPORT ISSUED MONTH August YEAR 1984
	6. (Leave blank)
	8. (Leave blank)
12. SPONSORING ORGANIZATION NAME AND MAILING ADDRESS (Include Zip Code) U.S. Nuclear Regulatory Commission Office of Nuclear Regulatory Research Washington, D. C. 20555	10. PROJECT/TASK/WORK UNIT NO.
	11. FIN NO. A2243
13. TYPE OF REPORT Annual Report	PERIOD COVERED (Inclusive dates) October 1982--September 1983
15. SUPPLEMENTARY NOTES	14. (Leave blank)

16. ABSTRACT (200 words or less)

This progress report summarizes work performed by the Argonne National Laboratory during the twelve months from October 1982 to September 1983 on long-term embrittlement of cast duplex stainless steels used in light-water reactors.

17. KEY WORDS AND DOCUMENT ANALYSIS

Cast stainless steels
Embrittlement behavior
Low-temperature aging
Phase precipitation and identification

17a. DESCRIPTORS

17b. IDENTIFIERS/OPEN-ENDED TERMS

18. AVAILABILITY STATEMENT	19. SECURITY CLASS (This report) Unclassified	21. NO. OF PAGES 32
	20. SECURITY CLASS (This page) Unclassified	22. PRICE $

NRC FORM 335 (11-81)